Coherent multi-channel ranging for precise localization in narrowband LPWA networks: performance trials in an indoor environment

Vincent Berg, Francois Dehmas, Florian Wolf

Coherent Multi-channel Ranging for Precise Localization in Narrowband LPWA Networks: Performance Trials in an Indoor Environment

Vincent Berg, François Dehmas and Florian Wolf
CEA-Leti, Université Grenoble Alpes, F-38000 Grenoble, France
Email: {vincent.berg, francois.dehmas, florian.wolf}@cea.fr

***Abstract*—Wearable health monitoring is a promising application where Low Power Wide Area (LPWA) connectivity and location services are required. LPWA radios are suited thanks to their small size, low power and low cost, while providing ubiquitous and indoor coverage. However, current LPWA applications do not provide accurate enough localization information for this application. Coherent multi-channel ranging has recently been proposed to improve localization precision. This paper studies the resilience of the new approach in an indoor environment. Field trials performed in office premises confirm the potential of the new technique where performance is significantly better than legacy time-of-flight even in this severe environment.**

***Index Terms*—Narrowband localization, LPWA, frequency hopping, indoor localization**

I. Introduction

Low Power Wide Area (LPWA) networks provide a promising communication technology that enable wireless connectivity on a large variety of Internet of Things (IoT) objects. Long range of connectivity is achieved thanks to low levels of receiver sensitivity obtained by low data rates and narrowband modulation schemes for both proprietary LPWA solutions such as Long Range from Semtech (LoRA) and standardized ones such as Narrow-Band IoT (NB-IoT). The demand for IoT is often tightly linked to its ability to provide, along with connectivity, location-based services: many IoT applications fundamentally depend on the location information to meaningfully interpret any physical measurements collected [1].

Wearable health monitoring, currently under study by the H2020 Project 5G-HEART [2], is one promising application where both standalone LPWA connectivity and location services should be provided. The health application has emerged as an effective way for improving the quality of life of the patient as it provides seamless remote monitoring and diagnostics. In this case, a wearable patch is used to monitor vital health signals. An emergency alert is triggered when patients suffering from critical conditions require immediate help. Examples include heart conditions, diabetes and epilepsy. Strong requirements to localize the patient are put on the patch for emergency services to effectively assign resources at the right location. The challenge for developing single-use, direct-to-cloud, vital-signs patches lies in enabling the required functionality in a very small form factor, whilst guaranteeing long battery life and low device cost [2]. LPWA radios and their 5G evolutions are suited for these applications thanks to their small size, low-power and low-cost, while providing "deep" indoor and ubiquitous coverage. LPWA does not require a high density of infrastructure, which is costly to deploy and maintain. Accurate localization of the patient is, however, essential to facilitate the work of emergency services. Global Navigation Satellite System (GNSS) solutions are unsuitable because of extra energy consumption and unavailability for indoor operation.

Current LPWA approaches do not however provide accurate enough localization ranging information to meet the requirements of the application in outdoor and indoor environments. Fingerprinting methods based on radio signal strength indications, although straightforward to implement, requires to construct and maintain large databases. Furthermore, errors are not smaller than $500\,\mathrm{m}$ in an urban environment [3]. Alternatively, Time of Flight (ToF) based localization is bound by the signal bandwidth used to estimate ranging information [4]. Accurate ToF requires accurate Time of Arrival (ToA) and is very challenging as narrowband modulation schemes are used. State-of-the-art Time-Difference-of-Arrival (TDoA) achieves $250\,\mathrm{m}$ accuracy in this context [5].

A new technique, called coherent multi-channel ranging, has therefore been proposed to significantly improve localization precision of narrowband signals. It relies on multiple narrowband signals that are sequentially transmitted on different and discontinuous channels to virtually increase the bandwidth of the transmitted signal [6][7]. This technique, based on multiple phase measurements or Phase of Flight (PoF), significantly improves temporal resolution and ranging precision, while preserving the narrowband modulation necessary for long-range communications. Performance evaluation of PoF measured through field trials has already proved its potential in an outdoor environment [7]. In a urban environment strong biases have been observed and a ranging bias estimator has been introduced to detect Non-Line-Of-Sight (NLOS) propagation conditions [7]. However, evaluation of performance of the PoF technique in an indoor environment has so far not being performed, this is however fundamental for the targeted wearable health monitoring application.

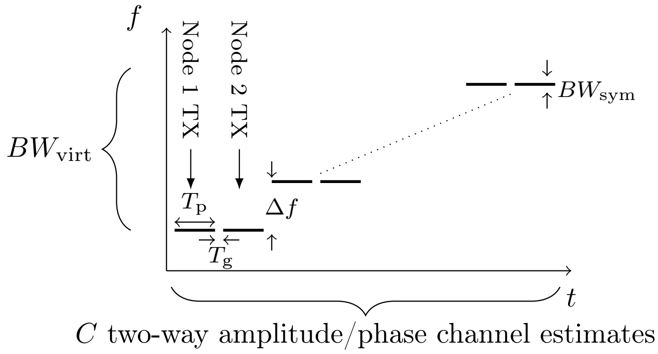

Fig. 1. Multi-channel ranging signaling process for C sequentially aggregated narrowband (BW_{sym}) channels.
The C channels form a virtual bandwidth equal to $BW_{\mathrm{virt}} = (C-1)\Delta f$.

This paper is organized as follows. Section II introduces the principles of PoF ranging and evaluates its associated performance in comparison to legacy ToF under Additive White Gaussian Noise (AWGN). The environment, set-up and performance results are then presented in Section III. Section IV concludes the paper.

II. Coherent Multi-Channel Ranging

A. Principles and derivation of PoF

Coherent Multi-Channel ranging relies on two nodes sequentially performing a two-way narrowband packet exchange on different carrier frequencies $f_c = f_{\mathrm{R}} + c\Delta f$, $c \in [0, C-1]$, where f_{R} is a constant carrier frequency, Δf the channel spacing and C the number of channels [7]. Fig. 1 gives a time-frequency representation of the associated signaling process. The two-way exchange is designed to remove synchronization constraints between both nodes.

The cross correlation of the received signal $r_c^{[X]}$ with the transmitted known preamble s_0 for both nodes $X \in \{R_1, R_2\}$ is given by:

$$\Omega^{[X]}_{r_c,s_0}[t_{\mathrm{A}}, \delta_{\mathrm{f_c}}] = \sum_{k=0}^{K_{\mathrm{S}}-1} \left(r_c^{[X]} \left[k - \frac{t_{\mathrm{A}}}{T_{\mathrm{S}}} \right] \right)^* s_0[k] \cdot e^{-j2\pi\delta_{\mathrm{f}} f_c k T_{\mathrm{S}}}, \tag{1}$$

with complex conjugate $(\cdot)^*$, sampling period T_{S} over K_{S} samples. For each channel c, estimates of the relative Carrier Frequency Offset (CFO), $\widehat{\delta_{\mathrm{f_c}}}^{[X]}$, the ToA $\widehat{t_{\mathrm{A_c}}}^{[X]}$, the Phase-of-Arrival (PoA) $\widehat{\phi_c}^{[X]}$ and the amplitude, $\widehat{A_c}^{[X]}$, are given according to [8] by:

$$\widehat{\delta_{\mathrm{f}c}}^{[X]} = \arg\max_{\delta_{\mathrm{f}}} \max_{t_{\mathrm{A}},\delta_{\mathrm{f}}} \left| \Omega^{[X]}_{r_c,s_0}[t_{\mathrm{A}}, \delta_{\mathrm{f}}] \right|, \tag{2a}$$

$$\widehat{t_{\mathrm{A}c}}^{[X]} = \arg\max_{t_{\mathrm{A}}} \max_{t_{\mathrm{A}},\delta_{\mathrm{f}}} \left| \Omega^{[X]}_{r_c,s_0}[t_{\mathrm{A}}, \delta_{\mathrm{f}}] \right|, \tag{2b}$$

$$\widehat{\phi_c}^{[X]} = \angle \left\{ \Omega^{[X]}_{r_c,s_0} \left[\widehat{t_{\mathrm{A}c}}^{[X]}, \widehat{\delta_{\mathrm{f}c}}^{[X]} \right] \right\}, \tag{2c}$$

$$\widehat{A_c}^{[X]} = \left| \Omega^{[X]}_{r_c,s_0} \left[\widehat{t_{\mathrm{A}c}}^{[X]}, \widehat{\delta_{\mathrm{f}c}}^{[X]} \right] \right|. \tag{2d}$$

The PoA estimates for the received signal from node 1 (resp. 2) at node 2 (resp. 1) are given by:

$$\phi_c^{[R_2]} = \phi_{\mathrm{R},c}^{[T_1]} - 2\pi f_c(\tau_0 + t_0) + \varphi_c - \phi_{\mathrm{R},c}^{[R_2]}, \tag{3a}$$

$$\phi_c^{[R_1]} = \phi_{\mathrm{R},c}^{[T_2]} - 2\pi f_c(\tau_0 - t_0) + \varphi_c - \phi_{\mathrm{R},c}^{[R_1]} + 2\pi f_c \delta_{\mathrm{f}}(T_{\mathrm{p}} + T_{\mathrm{g}} + \epsilon_t), \tag{3b}$$

with propagation delay τ_0, wireless propagation channel phase φ_c and initial transceiver oscillator phase $\phi_{\mathrm{R},c}^{[X]}$. The return packet in (3b) integrates a phase error introduced by the relative CFO, δ_{f}, at time $T_{\mathrm{p}} + T_{\mathrm{g}} + \epsilon_t$ after PoA $\phi_c^{[R_2]}$. This phase error can be corrected with a CFO estimation at the receiver and the a priori knowledge of $T_{\mathrm{p}}+T_{\mathrm{g}}$. CFO estimation precision should fulfill $\epsilon_{\delta_{\mathrm{f}}} < \epsilon_{\tau_0}/(T_{\mathrm{p}} + T_{\mathrm{g}})$, when maximum acceptable range error is ϵ_{τ_0}. The time synchronization error ϵ_t may be considered negligible as $\delta_{\mathrm{f}}\epsilon_t \ll \tau_0$. The time offset t_0 between both nodes is cancelled when combining (3a) and (3b) as Phase-of-Flight (PoF):

$$\phi_c^{[1,2]} = \phi_c^{[R_2]} + \phi_c^{[R_1]} = -4\pi f_c \tau_0 + 2\varphi_c + \Delta\phi_{\mathrm{R},c}, \tag{4}$$

with $\Delta\phi_{\mathrm{R},c} = \phi_{\mathrm{R},c}^{[T_1]} - \phi_{\mathrm{R},c}^{[R_2]} + \phi_{\mathrm{R},c}^{[T_2]} - \phi_{\mathrm{R},c}^{[R_1]}$. PoF imposes a transceiver architecture that ensures $\Delta\phi_{\mathrm{R},c} = \mathrm{const.}$ for all c.

In presence of multipath propagation, the compound channel transfer function is constructed as follows:

$$H_c = H(f)|_{(f=f_{\mathrm{R}}+c\Delta f)} = \widehat{A_c}^{[R_1]} \widehat{A_c}^{[R_2]} e^{j\widehat{\phi_c}^{[1,2]}}. \tag{5}$$

The inverse discrete Fourier transform (iDFT) is then applied to $\boldsymbol{H} = [H_0, \ldots, H_{C-1}]$ to derive the compound Channel Impulse Response (CIR), $h(\tau)$, of the transmission channel [8]. The range resolution for this scheme is function of the virtual bandwidth BW_{virt} and equal to $\Delta R = c_0/(2(C-1)\Delta f) = c_0/(2BW_{\mathrm{virt}})$ [4], where c_0 is the speed of light. In the presence of NLOS, ranging information between transceivers is often biased and the measure should be discarded. NLOS propagation is detected using a statistical estimate of the resulting compound CIR based on a measure of its delay spread:

$$\sigma_\tau = \sqrt{\overline{\tau^2} - \left(\overline{\tau^1}\right)^2}, \tag{6}$$

with first and second moment $\overline{\tau^1}$ and $\overline{\tau^2}$ of the amplitude CIR $|h(\tau)|$. The delay spread estimate is compared to a threshold ζ_{opt} to classify the nature of the propagation between Line-Of-Sight (LOS) or NLOS [9]. This metric has already been evaluated in an outdoor campus environment and proved very valuable [7]. However, the behavior and performance of the approach has not yet been evaluated in a severe indoor environment where multipath propagation is prevalent. This is particularly crucial for the Health applications explored by the 5G-HEART project where "deep" indoor communication is considered for the wearable health monitoring patch.

B. Performance in presence of AWGN

The principles of coherent multichannel ranging have been evaluated by numerical simulation under AWGN channel

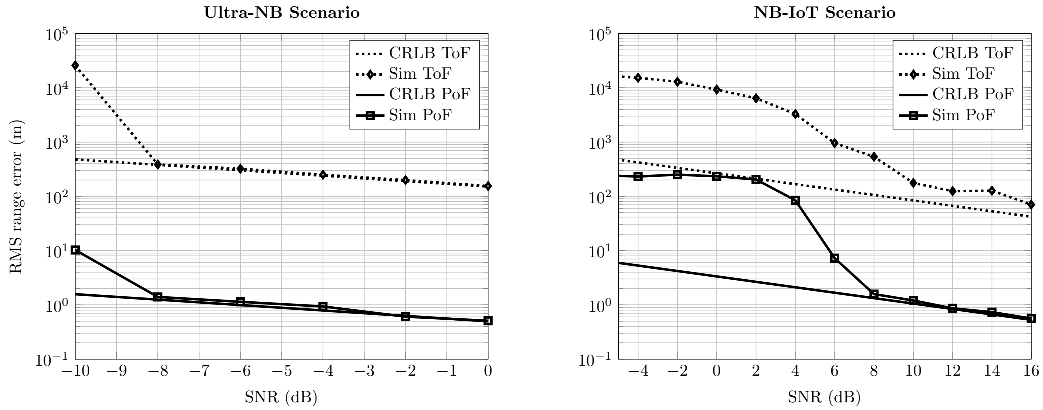

Fig. 2. Simulated performance for both scenarios, ultra-NB (left) and NB-IoT (right).

conditions and CFO in order to theoretically estimate the ranging performance of the algorithm and compare them to field measurements. Simulation performance results are given in Fig. 2. Two different signal scenarios have been considered, an ultra-narrowband (NB) scenario and an evolution of 5G-NB-IoT. In both cases two transceivers perform a multi-channel two-way ranging according to Fig. 1.

For the ultra-NB scenario, a 256-bit Gold code is modulated on a Binary Phase Shift Keying (BPSK) at a rate, $R_c = 10kb/s$ and repeated $C = 16$ times with a channel spacing $\Delta f = 200$kHz. For the NB-IoT scenario, it is assumed that signaling is transmitted over a NPUSCH channel modulated using a single carrier modulation ($\pi/2$-BPSK) at rate equal to 15kHz for the uplink and NPDSCH over 180kHz bandwidth for the downlink. The transmitted signal consists on a Barker sequence of $N_c = 7$ bits in order to fit the coded sequence within the duration of a NB-IoT frame slot. The transmitted sequence is repeated on $C = 16$ different frequencies with a channel spacing Δf equal to 180kHz. The complete localization signal could therefore be transmitted over one 15kHz single carrier NB-IoT frame (or approx. 16ms) when FDD is considered. This hypothesis is coherent with the low power application but requires a frequency hopping evolution in NB-IoT.

Scenario parameters are summarized in Table I and simulated performance is given in Fig. 2 along with the Cramer Rao Lower Bound (CRLB). The main difference between both scenarios comes from the sequence duration that has been considered as the CRLB is a function of the overall received signal energy. Since the virtual bandwidth, BW_{virt} is of the same order of magnitude, performance is dominated by the Signal to Noise Ratio (SNR) at the receiver.

III. Field Trial in indoor environment

A. Transceiver Testbed

An experimental transceiver testbed has been used for the indoor field trial (Fig. 3) [6][7]. It is built around a Software Defined Radio (SDR) that includes a radiofrequency (RF) front-end system-on-chip from Analog Devices (reference AD9361) and a Xilinx Zynq-045 Field Programmable Gate Array (FPGA) with integrated dual Cortex-A9 ARM processor. The electronic board is interfaced to a GNSS module to obtain a ground truth for outdoor measurements. For indoor measurements, laser ranging is used instead as ground truth. Digital intermediate frequency up-/down-mixing stages are implemented in digital in the FPGA. This allows coherently processing a $10\,\mathrm{MHz}$ bandwidth by sequentially selecting at the receiver $1\,\mathrm{MHz}$ channels. This architecture ensures that $\Delta\phi_{\mathrm{R},c}$ is constant for all channels c as required by (4).

Two transceiver testbeds perform a multi-channel two-way ranging protocol according to Fig. 1 and using the ultra-NB scenario parameters (see Table I). Transmit power is set to $P_{\mathrm{TX}} = 0\,\mathrm{dBm}$. Radio frequency filters and the circulator, connecting TX and RX to the same antenna, add an attenuation A_{RF} of approximately $5\,\mathrm{dB}$.

B. Field Trial measurements

Experimental measurements have been realized within the premises of CEA in Grenoble, France. Measurements have been taken place over two different days and two measurement campaigns. An overview plan of the measurement environment is given in Fig. 4. The Radio Frequency (RF) propagation environment is typical of office buildings. A base station (BS) is positioned outside the building (BS) and ranging

TABLE I
Waveform and Multi-Channel Ranging Scenario Parameters.

Parameter	Ultra-NB	NB-IoT
Sequence Type	Gold Code	Barker
Sequence Size	256 bits	7 bits
Narrow Bandwidth, BW_{sym}	10kHz	15kHz
Channel Spacing, Δf	200kHz	180kHz
Virtual Bandwidth, BW_{virt}	3MHz	2.7MHz
Sequence Duration	819ms	16ms
Range resolution, ΔR	50m	55m

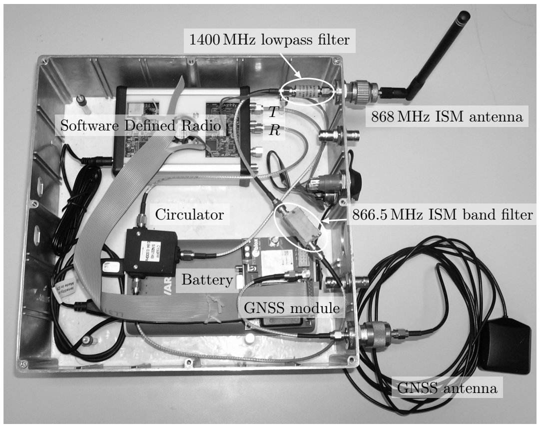

Fig. 3. Transceiver testbed composed of a SDR, radio frequency components, a GNSS module and a power supply.

measurements are performed along a planned path (put in green in Fig. 4). An optical laser ranging tool has been used to manually georeference ten reference points (from $\mathbf{P_0}$ to $\mathbf{P_9}$). These reference points are within the building premises and serve to evaluate the performance of the experimental coherent multi-channel ranging system in an indoor environment. The reference points are classified into two categories, LOS and NLOS depending on their ability to be in direct line-of-sight of the base station. $\mathbf{P_0}$ to $\mathbf{P_5}$ are considered to be in LOS and $\mathbf{P_6}$ to $\mathbf{P_9}$ in NLOS.

In order to validate the experimental setup, a first set of measurements is performed through a cable plant. Both transceivers are connected through a coaxial cable in order to evaluate and compare the experimental performance with the theoretical AWGN scenario simulated in Fig. 2. For this first set of measurements, the measured RMS range error is equal to 177m when legacy ToF is considered and equal to 2.6m when the new PoF metric is used. It should be noted that the mean and median values for the legacy ToF algorithm is significantly biased for all the experimental measurements. This could be attributed to the hardware setup and to the lack of accuracy of ToF when narrow bandwidth signals are considered. Performance has been reported as measured, however biases could be mitigated.

An overview of the statistic distribution of the measurement points is given in Fig. 5. Box-and-whisker plots have been used to anlayze the performance results. Each plot gives the minimum, the maximum, the sample median, and the first and third quartiles of the measured error. Performance errors are in line with the theoretical results of Fig. 2. Measured performance level in the field is comparable to simulated performance. This tends to suggest that RF and hardware impairments are second order for the targeted localization accuracy of $\sim$10 meters. Statistics of performance are also analyzed when NLOS detection is activated with a threshold ζ_{opt} set to 75m. This threshold has proven efficient for outdoor measurements [7].

Ranging measurements over the air are then performed and compared to their reference ranging value. A total of 2051 measurement points have thus been collected. Analysis is done separately for reference points that are in LOS (Fig. 6) from the base station to reference points that are in NLOS (Fig. 7). For the reference points identified in LOS, the measured RMS range error is equal to 181m and 3.8m for respectively legacy ToF and PoF. Furthermore, ranging error, once outliers are removed, lie within ± 10 meters. Half of the points are within ± 4 meters.

This tends to suggest that indoor propagation does not affect the performance of the coherent multi-channel ranging PoF algorithm. This result is significant as indoor propagation tends to spread the channel impulse response even when in LOS as reflections occur along the inside walls of the building and could cause severe degradation of performance. Degradation is expected to be further exacerbated by the fact that the instantaneous transmitted signal is very narrowband. Also note, that when in LOS, the NLOS detection criteria does not

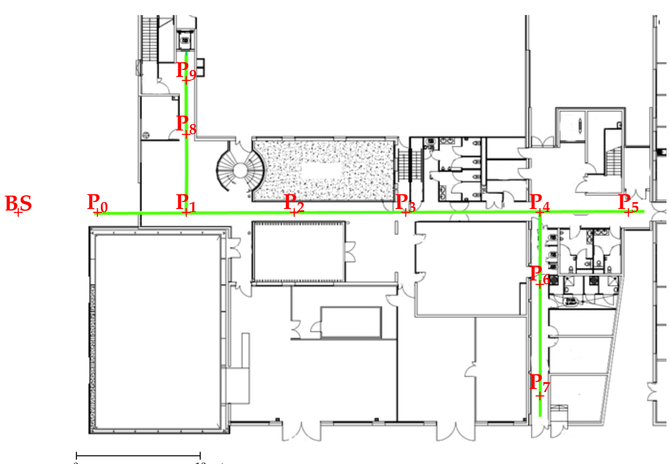

Fig. 4. Office building floor plan and field trial measurement points.

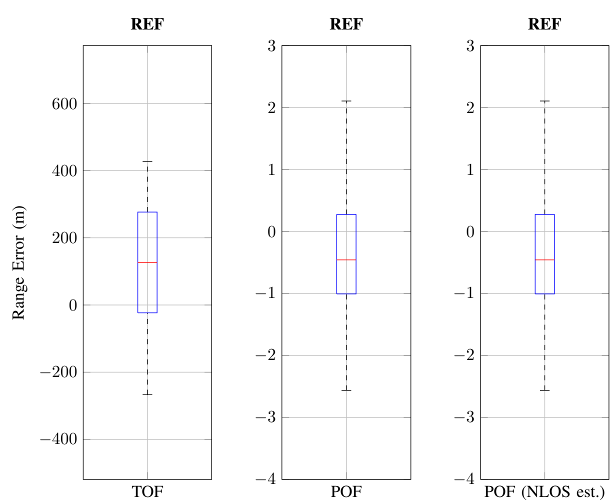

Fig. 5. Performance comparison through cable plant (AWGN).

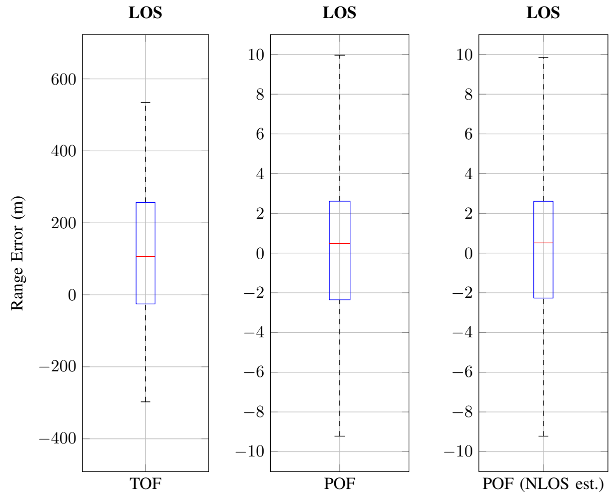

Fig. 6. Performance comparison for LOS reference points.

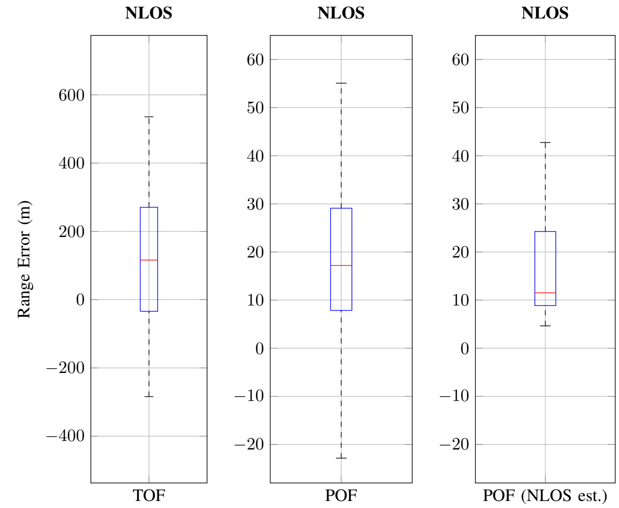

Fig. 7. Performance comparison for NLOS reference points

affect the statistics of the ranging performance, although 1.2% of PoF ranging measurements are detected as NLOS and thus would be potentially discarded by the localization solver.

For the reference points located in NLOS from the base station, the RF signal is transmitted through a non-direct path, hence the error introduced by the estimation technique is as expected significantly biased. For legacy ToF, the biases introduced by the multipath environment setup are well below the level of performance of the algorithm. Performance degradation is thus not observed. For the newly developed PoF algorithm, significant ranging error is observed, furthermore error is spread over a larger distance: for legacy ToF, the measured RMS Range error increases slightly to 188m, while PoF performance is much more degraded as error varies from approximately -24m to $+55$m. However, when the NLOS detector is activated, ranging error variations are significantly reduced. Ranging estimates vary from $+5$ to $+42$ meters, suggesting that transmission is dominated by a main indirect path. Furthermore, 48% of data measurement points are rejected by the NLOS detector.

IV. Conclusion

Coherent multi-channel ranging has been evaluated in an indoor environment and compared to simulated performance. Ranging precision is not degraded and consistent with simulated performance when propagation occurs in quasi LOS even for this type of (indoor) environment. Furthermore, when transmission is in NLOS performance is significantly biased due to the non-direct propagation path. However, variance of signal measurement is significantly improved in comparison to legacy ToF ranging metrics. This paper thus confirms the potential of the new technique for the wearable health scenario considered in the H2020 5G-HEART project. Furthermore, the concept is fairly flexible and could be advantageously adapted to 5G-NB-IoT evolution as long as frequency hopping mechanisms could be considered. Future work includes more extensive field trials comprising kilometer-level inter-node range estimations.

Acknowledgment

This work was supported by the European Union's Horizon 2020 research and innovation programme under 5G-HEART project (grant agreement No 857034).

References

[1] R. C. Shit, S. Sharma, D. Puthal, and A. Y. Zomaya, "Location of Things (LoT): A Review and Taxonomy of Sensors Localization in IoT Infrastructure," *IEEE Communications Surveys Tutorials*, vol. 20, no. 3, pp. 2028–2061, 2018.

[2] P. H. Lehne *et al.*, "D3.1: Healthcare Vertical Trial Requirements Definition and Execution," 5GHEART deliverable, Tech. Rep., October 2019.

[3] M. Aernouts, B. Bellekens, R. Berkvens, and M. Weyn, "A Comparison of Signal Strength Localization Methods with Sigfox," in *2018 15th Workshop on Positioning, Navigation and Communications (WPNC)*, Oct 2018, pp. 1–6.

[4] M. Skolnik, *Radar Handbook*, 2nd ed. McGrawHill, 1990.

[5] N. Podevijn, D. Plets, J. Trogh, L. Martens, P. Suanet, K. Hendrikse, and W. Joseph, "TDoA-Based Outdoor Positioning with Tracking Algorithm in a Public LoRa Network," *Wireless Communications and Mobile Computing*, 2018.

[6] F. Wolf, J. Doré, X. Popon, S. d. Rivaz, F. Dehmas, and J. Cances, "Coherent Multi-Channel Ranging for Narrowband LPWAN: Simulation and Experimentation Results," in *2018 15th Workshop on Positioning, Navigation and Communications (WPNC)*, 2018, pp. 1–6.

[7] F. Wolf, S. de Rivaz, F. Dehmas, V. Mannoni, V. Berg, and J. P. Cances, "Accurate Narrowband LPWA Ranging: Principles, Performance in AWGN and Multipath Channels," in *2020 European Conference on Networks and Communications (EuCNC)*, 2020, pp. 149–153.

[8] M. Pichler, S. Schwarzer, A. Stelzer, and M. Vossiek, "Multi-Channel Distance Measurement With IEEE 802.15.4 (ZigBee) Devices," *IEEE Journal of Selected Topics in Signal Processing*, vol. 3, no. 5, pp. 845–859, Oct 2009.

[9] S. Marano, W. M. Gifford, H. Wymeersch, and M. Z. Win, "NLOS Identification and Mitigation for Localization based on UWB Experimental Data," *IEEE Journal on Selected Areas in Communications*, vol. 28, no. 7, pp. 1026–1035, Sep. 2010.